

# Acetylcholine Detection Based on pH-Sensitive Liposomes

Min Kyeong Kang and Jin-Won Park\*

Cite This: *ACS Omega* 2021, 6, 14963–14967

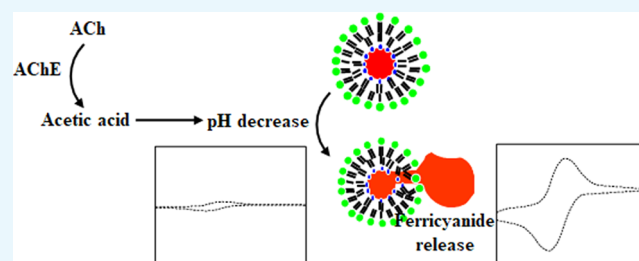
Read Online

ACCESS |

Metrics &amp; More

Article Recommendations

**ABSTRACT:** The pH-sensitive liposomes were employed to amplify the detection of acetylcholine (ACh). Acetylcholinesterase (AChE) covalently immobilized on the magnetic particles and the pH-sensitive liposomes encapsulating ferricyanide were added to a cyclic voltammetry cell solution where ACh was distributed. The conversion of ACh into acetic acid seemed to induce the pH decrease that caused the reduction in the electrostatic repulsion between the head groups of weakly acidic 1,2-dipalmitoyl-*sn*-glycero-3-succinate. The reduction generated liposome destabilization, which released potassium ferricyanide encapsulated inside the liposomes. The effects of the ACh concentration and pH were investigated. An addition of 10  $\mu\text{L}$  of more than 0.5 mg/mL ACh concentration into 5 mL of a cyclic voltammetry cell solution was necessary to observe the response. The activity of AChE was reversible with respect to the pH change between 7 and 5. The sensitivity of this detection was almost identical to comparable techniques such as enzyme-linked immunosorbent assay, field-effect transistor, fluorescence, UV spectrometry, magnetic resonance imaging, and surface plasmon resonance. Therefore, the methodology developed in this study is feasible as a portable, rapid, and sensitive method.



## 1. INTRODUCTION

Acetylcholine (ACh) is a neurotransmitter that functions in the brain and body of many types of animals and human beings and is released by nerve cells to send signals to other cells, such as neurons, muscle cells, and gland cells.<sup>1</sup> Since the abnormal levels of acetylcholine are related to dyskinesias, Parkinson's disease, and visual hallucinations, it has been pursued to achieve highly sensitive and specific techniques to detect the ACh concentration.<sup>2–4</sup> The analytical techniques including capillary electrophoresis, enzyme-linked immunosorbent assay, field-effect transistor, and liquid chromatography have been developed for the detection.<sup>5–8</sup> However, these techniques have drawbacks such as accessibility, time-lapse, or high cost. Since faster diagnosis generally leads to better prognosis, much effort has been made to overcome the limitations. Recently, different portable detection strategies have been developed.<sup>9–14</sup>

The pH-sensitive liposomes have a spherical lipid bilayer that can be destabilized when the external pH is changed, usually from a neutral or slightly alkaline pH to an acidic pH. The liposomes are designed to release the contents inside them, which are proteins and peptides, oligonucleotides, carbohydrate, inorganic carrier, antisense strands, plasmids, contrast agent, and antibodies and drugs.<sup>15–19</sup> The advantages of liposomes are simplicity of preparation, biocompatibility, versatility of surface modification, operability of dimensional control, and large-volume internal loading. Therefore, numerous pH-sensitive liposomes have been developed for

each mechanism. Liposomes are prepared mainly with phosphatidylethanolamine (PE), whose structure is a favorable shape for the formation of a hexagonal phase. Destabilization requires the inclusion of a weakly acidic amphiphile such as cholesterylhemisuccinate (CHEMS), phosphatidylserine (PS), and phosphatidylglycerol (PG) that are used to stabilize the liposomes at neutral pH.<sup>20</sup> The electrostatic repulsion between the head groups of these amphiphiles keeps the structure of the liposomes intact. When the liposomes with PE and the weakly acidic amphiphile are immersed in an acidic environment, they are destabilized.<sup>21</sup>

The hydrolysis of ACh leads to the production of acetic acid and choline, which results in the reduction of the pH value.<sup>22</sup> The reduction can be used to stimulate the change in the response. However, since the  $pK_a$  value of acetic acid is around 4.8, the change is little remarkable, though clearly distinguishable, especially under an atmospheric environment including carbon dioxide.<sup>23</sup> Carbon dioxide is capable of decreasing the pH value to even lower than 5.5. Therefore, pH sensitivity may be considered for the amplification of the minute response. In this work, we aim to develop a portable, rapid, and sensitive

Received: February 24, 2021

Accepted: May 14, 2021

Published: June 7, 2021



method to detect ACh with pH-sensitive liposomes. The pH change from ACh triggers the release of the liposomal contents around the electrodes, which are the electrons dissociated from the contents according to the applied voltage rate.

## 2. RESULTS AND DISCUSSION

The immobilization of AChE was confirmed using X-ray photoelectron spectroscopy (XPS). After each step of immobilization, the surface was analyzed in terms of elements that have their own binding energies (Table 1). The relative

**Table 1. XPS Results for Each Step of AChE Immobilization on Magnetic Particles**

	silicon oxide (%)	PEI treatment (%)	glutaraldehyde treatment (%)	AChE immobilization (%)
C 1s	0.1	19.0	23.8	26.7
N 1s	0.1	8.0	6.0	7.3
O 1s	67.5	50.0	48.9	46.4
Si	32.3	23.0	21.3	19.4
2p				
S 2p				0.2

amount of each element was represented by the peak distribution of the energy. Prior to any treatment, the peaks of silicon and oxygen only were found on the surface of the silicon wafer. After poly(ethyleneimine) (PEI) coating, the amount of carbon and nitrogen increased tremendously. This increase indicated that the surface was coated successfully with PEI. The changes in the amounts, led by the glutaraldehyde reaction and AChE immobilization as next steps, were expected. The results of XPS were consistent with that of previous research.<sup>24</sup>

The response of the pH-sensitive liposome was monitored prior to the addition of both ACh and AChE, depending on the change in the pH value from 7 to 5 by 0.5. Then, the concentration of the liposome solution was also varied from 0.5 to 5 mg/mL. At pH 7–5.5, the difference in the spectra was indistinguishable, while a significant change occurred at pH 5.5–5 (Figure 1). This trend was identical at all

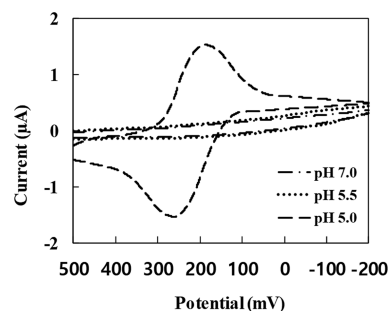


**Figure 1.** Cyclic voltammetry (CV) responses only for pH-sensitive liposomes encapsulating ferricyanide at different pH values.

concentrations, although the intensities of the measured currents were different. The intensity was linearly proportional to the concentration of the liposome, as shown in Figure 2. Since the liposome solution was not very stable to prepare reproducibly more than 5 mg/mL, the pH dependency was investigated up to 5 mg/mL. This dependency was interpreted with respect to the dissociation constant of 1,2-dipalmitoyl-*sn*-glycero-3-succinate (DPGS), which was around 5.4.<sup>25</sup> The pH

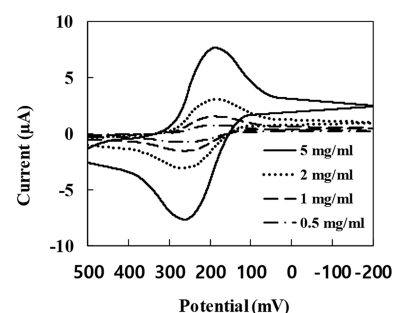


**Figure 2.** Cyclic voltammetry responses only for pH-sensitive liposomes encapsulating ferricyanide at different liposome concentrations at pH 5.

value less than 5.4 led to a decrease in the repulsion between the head groups of the lipids, and then liposomes were believed to release potassium ferricyanide to provide the signal (Figure 3).

The current responses were continuously monitored after the stepwise addition of following components. Prior to all of the additions, the standard cyclic voltammetry (CV) curve was confirmed with 1 mM potassium ferricyanide. The additions were performed in the order of AChE-immobilized magnetic particle solution, ACh solution, and pH-sensitive liposome solution, respectively. The responses were acquired before and after the addition of the pH-sensitive liposome solution, as suggested in Figure 4. The liposome concentration in the CV cell solution was 1 mg/mL. The response before liposome addition was almost identical to that of the insulated electrode, although no treatment was performed on the electrode surface.<sup>26</sup> This result indicated that ACh and AChE by themselves are little involved in the electrolyte transport. After the addition of liposome solution, the response was increased significantly. Obviously, this increase was caused by the liposome addition. However, it was essential to confirm whether the liposome addition by itself caused the increase or not. Therefore, only liposome solution was added to the CV solution without AChE-immobilized magnetic particles and AChs. The response with only liposomes was found identical with that of the insulated electrode.

For comparison, the addition of AChE-immobilized magnetic particles and the ACh solution into the cell was alternately excluded on purpose. This comparison was believed to provide insight into the role of the additions. As expected, without one of the additions, a slight increase in the response was observed, as that found prior to the addition of the pH-sensitive liposome. Therefore, it was concluded that the increase in response in the presence of AChE-immobilized magnetic particles, AChs, and pH-sensitive liposomes seems to be generated by the relation among AChE, ACh, and liposomes. Furthermore, it was essential to clarify whether this relation was through the change in pH. Therefore, instead of pH-sensitive liposomes, pH-insensitive liposomes made with only 1,2-dipalmitoyl-*sn*-glycero-3-phosphocholine (DPPC) were added. The response of the liposomes with only DPPC was clearly different from that of pH-sensitive liposomes and almost identical to that of the missing one of the three additions. Therefore, the relation among AChE, ACh, and the pH-sensitive liposomes, generating a significant increase in the response, was based on pH.

After the proof of the working principle, the dependency of the ACh concentration on the response was investigated in a 1

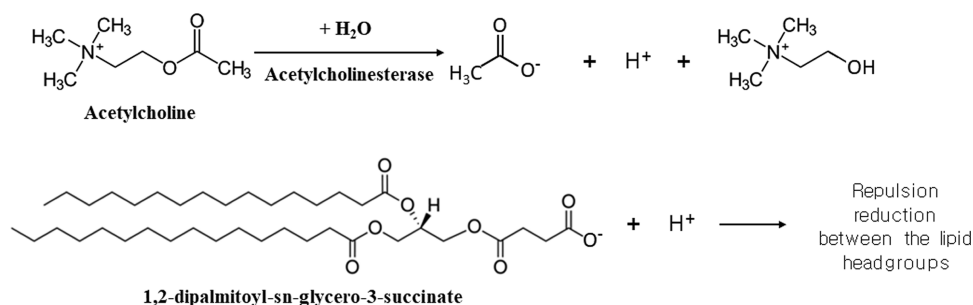


**Figure 3.** Schematic diagram of the phenomena after acetylcholine, acetylcholinesterase, and pH-sensitive liposome injection – decomposition of acetylcholine and the effect of proton production.

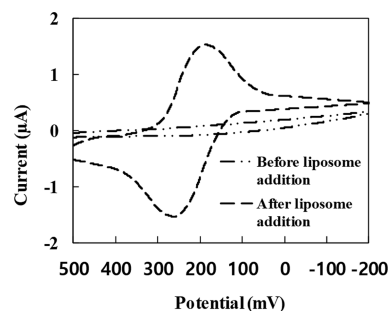


**Figure 4.** Cyclic voltammety responses before and after the addition of pH-sensitive liposomes into the solution including AChE-immobilized magnetic particles and ACh.

mg/mL pH-sensitive liposome solution. Ten microliters of the ACh solution at 0.1, 0.2, 0.5, and 1.0 mg/mL concentration was injected into the cells. No change in the response was observed at the former two concentrations, while an identical change was found at the latter concentrations (Figure 5).

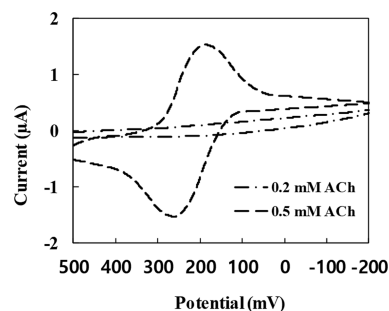


**Figure 5.** Cyclic voltammety responses on the ACh concentration in a 1 mg/mL pH-sensitive liposome solution.

These results were interpreted with respect to the pH effect, which was related to the product from ACh. The concentration was validated using commercial colorimetry. If the concentration of ACh was low, the reactants for the hydrolysis seemed to be less to generate protons that would eventually induce the rupture of pH-sensitive liposomes. However, at 0.5 mg/mL or

more, it was believed that the liposomes released ferricyanide. Although more than 0.5 mg/mL might generate more protons, the change in the liposome structure ultimately occurred with a concentration equal to 0.5 mg/mL. Regarding the response on the ACh concentration, the dissociation constant of DPSG was also critical for the results with respect to the change in pH value.

The sensitivity of the detection based on the pH-sensitive liposomes was estimated. Since the response was observed at even 5 mL of the cell solution, into which 10 µL of 0.5 mg/mL ACh was injected, the sensitivity was estimated at around 10 nM concentration. The limit of detection was 10 nM because the liposome concentration has a limitation of 0.5 µg/mL and the CV current has 10 pA accuracy. This limitation was found to be similar to comparable techniques such as ELISA, FET, fluorescence, UV spectrometry, magnetic resonance imaging, and surface plasmon resonance.<sup>8,27–31</sup> The reversibility of the AChE activity on the pH value was found to be in the range of 7.0–5.0, where the pH of the cell solution continuously changed, which was found to be identical with the previous results.<sup>32</sup> The selectivity to other neurotransmitters was also important. The detection based on the pH-sensitive liposomes was tested in a mixture of ACh, dopamine, and serotonin. In the mixture solution, each component was at 1 mg/mL concentration, much higher than the typical concentration.<sup>33</sup> The response of the mixture was little different from that of the pure ACh compared with the mixture without ACh.

### 3. EXPERIMENTAL SECTION

Acetylcholinesterase (AChE) was immobilized on magnetic particles through covalent links (Figure 6). A 150 µL aliquot of a stock solution, containing 3 µm diameter particles from Bang Lab (Fisher, IN) was washed three times with 50 mM carbonate buffer, pH 8.2. The particles were coated with 3% (w/v) PEI in 2 mL of 50 mM carbonate buffer, pH 8.2, for 1 h, separated magnetically from the PEI solution, and resuspended by vortexing. The particles were thoroughly washed with 20 mM *N*-(2-hydroxyethyl)piperazine-*N'*-ethanesulfonic acid (HEPES), 150 mM NaCl, and 5 mM CaCl<sub>2</sub> (pH 7.4), and functionalized by reacting with 2.5% (v/v) glutaraldehyde in

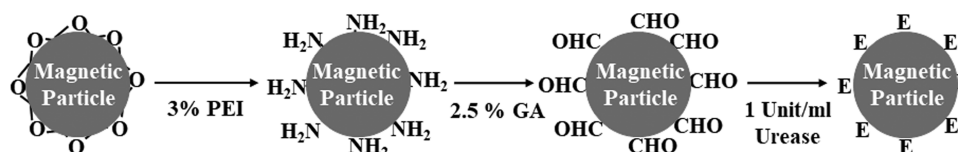


**Figure 6.** Scheme used to immobilize acetylcholinesterase on magnetic particles, GA and E indicate glutaraldehyde and acetylcholinesterase.

the HEPES buffer solution for 45 min with PEI coated on them. The particles were immersed in 50 mL of the HEPES buffer solution containing 50 U of AChE (Sigma, St. Louis, MO) for 3 h. For the confirmation of the AChE immobilization, X-ray photoelectron spectroscopy (PHI 5800, Physical Electronics, Inc., Chanhassen, MN) spectra were obtained. The spectra were recorded on the particles adsorbed physically on a silicon wafer (Sehyung Wafer Tech., Seoul, S. Korea) and treated with the identical procedures described above. Using the Bradford reagent, the concentrations of the injected and unbound enzymes were found. Therefore, the concentration of the immobilized enzyme was estimated at about 1.0  $\mu\text{M}$  and 8.0 ng protein/mg particle.

For the pH-sensitive liposome preparation, 1,2-dipalmitoyl-*sn*-glycero-3-phosphocholine (DPPC) and 1,2-dipalmitoyl-*sn*-glycero-3-succinate (DPGS) from Avanti were dissolved in a 60:40 ratio (DPPC/DPGS) or pure DPPC in chloroform. Chloroform was subsequently evaporated at 50 °C under a dry stream of nitrogen to form lipid films on the inner wall of a glass tube. The inner wall was kept at low pressure for several hours to remove last traces of the solvent and immersed overnight at room temperature in 2 mL of the HEPES buffer solution containing 1 mM potassium ferricyanide ( $\text{K}_3\text{Fe}[\text{CN}]_6$ ). The film-suspended solution was subjected to freezing and thawing with vigorous vortexing every 10 min for 10 cycles, and to extrusion of two-stacked 100 nm pore size polycarbonate filters at 50 °C to obtain unilamellar liposomes. The liposome solution was transferred to a dynamic light scattering instrument (ELS-8000, Otsuka, Tokyo, Japan) to measure the diameter of the liposomes, which was 150 nm on average with normal distribution ranging from 130 to 170 nm.

Cyclic voltammetry (CV) experiments were conducted with a CHI660B electrochemical workstation (CH Instruments Inc., Austin, TX). Five milliliters of the HEPES buffer solution where the AChE-immobilized particles were dispersed uniformly was transferred into the conventional Pyrex glass cell. A Ag/AgCl reference electrode, a Pt wire counter electrode, and a glassy carbon working electrode were immersed in the buffer solution. Then, 10  $\mu\text{L}$  of 0.5 mM ACh was injected into the solution in the cell, followed by the current measurements. The current was measured before and after the injection of the pH-sensitive liposomes described above. The potential was cycled ranging from 500 to  $-200$  mV relative to the reference electrode at a scan rate of 0.05 mV/s. The whole experiment was repeated three times, and the enzymes were separated from the CV cell solution using magnetic forces. For the confirmation of the abovementioned approach, commercial colorimetry was used. The calibration curve was acquired using solutions with known choline concentrations.

#### 4. CONCLUSIONS

In this study, the detection of ACh was amplified through the pH-sensitive liposomes. ACh detection was based on the conversion of ACh into acetic acid. The conversion occurred after the addition of ACh into the CV cell solution where the AChE-immobilized magnetic particles were dispersed. Acetic acid seemed to induce the pH decrease that caused the reduction in the electrostatic repulsion between the head groups of weakly acidic DPGS. The reduction generated liposome destabilization, which released potassium ferricyanide encapsulated inside the liposomes.

After the proof of the detection concept, the effects of the ACh concentration and the pH value were investigated. An addition of 10  $\mu\text{L}$  of more than 0.5 mg/mL ACh concentration into 5 mL of the CV cell solution was necessary to observe the response. The reversibility of AChE was maintained with respect to the pH change between 7 and 5. The sensitivity of this detection was almost identical with the comparable techniques such as enzyme-linked immunosorbent assay and field-effect transistor. Therefore, the technique developed in this study is feasible as a portable, rapid, and sensitive method.

#### ■ AUTHOR INFORMATION

##### Corresponding Author

**Jin-Won Park** – Department of Chemical and Biomolecular Engineering, College of Energy and Biotechnology, Seoul National University of Science and Technology, Seoul 01811, Republic of Korea; [orcid.org/0000-0003-4648-9692](https://orcid.org/0000-0003-4648-9692); Phone: +82-2-970-6605; Email: [jwpark@seoultech.ac.kr](mailto:jwpark@seoultech.ac.kr); Fax: +82-2-977-8317

##### Author

**Min Kyeong Kang** – Department of Chemical and Biomolecular Engineering, College of Energy and Biotechnology, Seoul National University of Science and Technology, Seoul 01811, Republic of Korea

Complete contact information is available at:  
<https://pubs.acs.org/10.1021/acsoomega.1c01023>

##### Notes

The authors declare no competing financial interest.

#### ■ ACKNOWLEDGMENTS

This study was supported by the Research Program funded by the SeoulTech (Seoul National University of Science and Technology).

#### ■ REFERENCES

- (1) Tiwari, P.; Dwivedi, S.; Singh, M. P.; Mishra, R.; Chand, A. Basic and modern concepts on cholinergic receptor: A review. *Asian Pac. J. Trop. Dis.* **2012**, *3*, 413–420.
- (2) Bohnen, N. I.; Albin, R. L. The Cholinergic System and Parkinson Disease. *Behav. Brain Res.* **2011**, *221*, 564–573.
- (3) Leino, S.; Kohtala, S.; Rantamaki, T.; Koski, S. K.; Rannanpaa, S.; Salminen, O. Dyskinesia and brain-derived neurotrophic factor levels after long-term levodopa and nicotinic receptor agonist treatments in female mice with near-total unilateral dopaminergic denervation. *BMC Neurosci.* **2018**, *19*, No. 77.
- (4) Esmaeeli, S.; Murphy, K.; Swords, G. M.; Ibrahim, B. A.; Brown, J. W.; Llano, D. A. Visual hallucinations, thalamocortical physiology and Lewy body disease: A review. *Neurosci. Biobehav. Rev.* **2019**, *103*, 337–351.
- (5) Andreescu, S.; Marty, J. L. Twenty years research in cholinesterase biosensors: from basic research to practical applications. *Biomol. Eng.* **2006**, *23*, 1–15.
- (6) Sangubotla, R.; Kim, J. Recent trends in analytical approaches for detecting neurotransmitters in Alzheimer's disease. *TrAC, Trends Anal. Chem.* **2018**, *105*, 240–250.
- (7) Kovarik, Z.; Radić, Z.; Berman, H. A.; Simeon-Rudolf, V.; Reiner, E.; Taylor, P. Acetylcholinesterase active centre and gorge conformations analysed by combinatorial mutations and enantiomeric phosphonates. *Biochem. J.* **2003**, *373*, 33–40.
- (8) Fenoy, G. E.; Marmisolle, W. A.; Azzaroni, O.; Knoll, W. Acetylcholine biosensor based on the electrochemical functionalization of graphene field-effect transistors. *Biosens. Bioelectron.* **2020**, *148*, No. 111796.

- (9) Yu, Z.; Cai, G.; Liu, X.; Tang, D. Pressure-Based Biosensor Integrated with a Flexible Pressure Sensor and an Electrochromic Device for Visual Detection. *Anal. Chem.* **2021**, *93*, 2916–2925.
- (10) Huang, L.; Chen, J.; Yu, Z.; Tang, D. Self-Powered Temperature Sensor with Seebeck Effect Transduction for Photo-thermal–Thermoelectric Coupled Immunoassay. *Anal. Chem.* **2020**, *92*, 2809–2814.
- (11) Yu, Z.; Tang, Y.; Cai, G.; Ren, R.; Tang, D. Paper Electrode-Based Flexible Pressure Sensor for Point-of-Care Immunoassay with Digital Multimeter. *Anal. Chem.* **2019**, *91*, 1222–1226.
- (12) Yu, Z.; Cai, G.; Tong, P.; Tang, D. Saw-Toothed Micro-structure-Based Flexible Pressure Sensor as the Signal Readout for Point-of-Care Immunoassay. *ACS Sens.* **2019**, *4*, 2272–2276.
- (13) Ren, R.; Cai, G.; Yu, Z.; Zeng, Y.; Tang, D. Metal-Polydopamine Framework: An Innovative Signal-Generation Tag for Colorimetric Immunoassay. *Anal. Chem.* **2018**, *90*, 11099–11105.
- (14) Zeng, R.; Tao, J.; Tang, D.; Knopp, D.; Shu, J.; Cao, X. Biometric-based tactile chemomechanical transduction: An adaptable strategy for portable bioassay. *Nano Energy* **2020**, *71*, No. 104580.
- (15) Slepushkin, V. A.; Simões, S.; Dazin, P.; Newman, M. S.; Guo, L. S.; de Lima, M. C. P.; Düzgüne, N. Sterically stabilized pH-sensitive liposomes intracellular delivery of aqueous contents and prolonged circulation in vivo. *J. Biol. Chem.* **1997**, *272*, 2382–2388.
- (16) Cai, G.; Yu, Z.; Tong, P.; Tang, D. Ti<sub>3</sub>C<sub>2</sub> MXene quantum dot-encapsulated liposomes for photothermal immunoassays using a portable NIR imaging camera on a smartphone. *Nanoscale* **2019**, *11*, 15659–15667.
- (17) Lin, Y.; Zhou, Q.; Zeng, Y.; Tang, D. Liposome-coated mesoporous silica nanoparticles loaded with L-cysteine for photo-electrochemical immunoassay of aflatoxin B1. *Microchim. Acta* **2018**, *185*, No. 311.
- (18) Ren, R.; Cai, G.; Yu, Z.; Tang, D. Glucose-loaded liposomes for amplified colorimetric immunoassay of streptomycin based on enzyme-induced iron(II) chelation reaction with phenanthroline. *Sens. Actuators, B* **2018**, *265*, 174–181.
- (19) Lin, Y.; Zhou, Q.; Tang, D. Dopamine-Loaded Liposomes for in-Situ Amplified Photoelectrochemical Immunoassay of AFB<sub>1</sub> to Enhance Photocurrent of Mn<sup>2+</sup>-Doped Zn<sub>3</sub>(OH)<sub>2</sub>V<sub>2</sub>O<sub>7</sub> Nanobelts. *Anal. Chem.* **2017**, *89*, 11803–11810.
- (20) Ferreira, D. D. S.; Lopes, S. C.; Franco, M. S.; Oliveira, M. C. pH-sensitive liposomes for drug delivery in cancer treatment. *Ther. Delivery* **2013**, *4*, 1099–1123.
- (21) Drummond, D. C.; Zignani, M.; Leroux, J. Current status of pH-sensitive liposomes in drug delivery. *Prog. Lipid Res.* **2000**, *39*, 409–460.
- (22) Hestrin, S. The reaction of acetylcholine and other carboxylic acid derivatives with hydroxylamine, and its analytical application. *J. Biol. Chem.* **1949**, *180*, 249–261.
- (23) Haynes, W. M. *CRC Handbook of Chemistry and Physics*, 97th ed.; CRC Press: New York, 2016.
- (24) Park, J.-W. Phosphatidic Acid Production by PLD Covalently Immobilized on Porous Membrane. *Clean Technol.* **2015**, *21*, 224–228.
- (25) Kashiwada, A.; Tsuboi, M.; Mizuno, T.; Nagasaki, T.; Matsuda, K. Target-selective vesicle fusion system with pH-sensitivity and responsiveness. *Soft Matter* **2009**, *5*, 4719–4725.
- (26) Lee, S. R.; Park, J.-W. Trehalose-Induced Variation in Physical Properties of Fluidic Lipid Bilayer. *J. Membr. Biol.* **2018**, *251*, 705–709.
- (27) Martino, G.; Twaddle, G.; Brambilla, E.; Grimaldi, L. M. E. Detection of anti-acetylcholine receptor antibody by an ELISA using human receptor from a rhabdomyosarcoma cell line. *Acta Neurol. Scand.* **1994**, *89*, 18–22.
- (28) Jin, T. Near-Infrared Fluorescence Detection of Acetylcholine in Aqueous Solution Using a Complex of Rhodamine 800 and p-Sulfonato-calix[8] arene. *Sensors* **2010**, *10*, 2438–2449.
- (29) Jones, R. S.; Stutte, C. A. Chromatographic analysis of choline and acetylcholine by UV visualization. *J. Chromatogr.* **1985**, *319*, 454–460.
- (30) Luo, Y.; Kim, E. H.; Flask, C. A.; Clark, H. A. Nanosensors for the Chemical Imaging of Acetylcholine Using Magnetic Resonance Imaging. *ACS Nano* **2018**, *12*, 5761–5773.
- (31) Kant, R.; Gupta, B. D. Fiber-Optic SPR Based Acetylcholine Biosensor Using Enzyme Functionalized Ta<sub>2</sub>O<sub>5</sub> Nanoflakes for Alzheimer's Disease Diagnosis. *J. Lightwave Technol.* **2018**, *36*, 4018–4024.
- (32) Bergmann, F.; Rimon, S.; Segal, R. Effect of pH on the activity of eel esterase towards different substrates. *Biochem. J.* **1958**, *68*, 493–499.
- (33) Mitchell, K. M. Acetylcholine and choline amperometric enzyme sensors characterized in vitro and in vivo. *Anal. Chem.* **2004**, *76*, 1098–1106.